communications earth & environment

Article

A Nature Portfolio journal

https://doi.org/10.1038/s43247-025-03142-y

Climate change has increased crop water consumption in Central Asia despite less water-intensive cropping

Mayra Daniela Peña-Guerrero [1,2,3,4] ✉, Gabriel B. Senay[5], Atabek Umirbekov[2,3,4], Larisa Tarasova [1], Philippe Rufin [3,6], Bakhtiyor Pulatov[7] & Daniel Müller [2,3,8]

Climate change and land use change are crucial determinants of crop water consumption, particularly in drylands where water scarcity limits crop production. In Central Asia, the effects of land use and climate changes on crop water consumption remain unknown. We estimated the dynamics of crop water consumption by mapping annual actual evapotranspiration from Landsat imagery from 1987 to 2019 for all irrigated croplands in the Amu Darya Basin, the largest transboundary river in Central Asia. Total crop water consumption increased by 10%, while average consumption per unit area increased by 18%. Climate change was the main driver of the rising crop water consumption; land use changes towards less water-intensive cropping practices offset only 3% of this increase. Our findings underscore that crop production will become increasingly challenging amidst accelerating climatic changes and that changing cropping practices alone will be insufficient to curb the growing water scarcity without a global commitment to reducing emissions.

Irrigated agriculture accounts for over 70% of global freshwater withdrawals and more than 90% of consumptive water use[1,2]. Increasing temperatures due to climate change elevate evapotranspiration, which raises crop water consumption and reduces water availability for irrigation[3,4]. Globally, the top 10% of most water-stressed river basins encompass 35% of the global irrigated calorie production[5]. Amidst accelerating climate change, monitoring the dynamics of crop water consumption and disentangling its drivers is key to securing livelihoods and food security, especially in water-scarce drylands where agriculture relies on irrigation.

In arid and semiarid basins, actual evapotranspiration (ETa) is the dominant outgoing flux of the water budget and therefore proxies crop water consumption in areas dominated by crop production[6–8]. Due to its close association with soil moisture, vegetative health, and atmospheric demand, ETa is a valuable indicator of landscape response to environmental and climatic drivers[9]. Quantifying ETa over space and time permits assessing crop water consumption and crop health and outlining the pathways for adaptation of crop production to climate change.

The endorheic river basins of Central Asia are particularly susceptible to climate change due to their highly continental and semi-arid climate, where evaporation dominates the water cycle[10,11]. Human interventions have further intensified pressure on water resources. Large-scale irrigation projects initiated during the Soviet period (1950s–1991) to achieve self-sufficiency in water-intensive cotton production led to the desiccation and salinization of the Aral Sea, once the world's fourth-largest inland water body[12,13]. Since the collapse of the Soviet Union, crop production in Central Asia has gradually shifted away from cotton to less water-intensive winter wheat; concurrently, double-cropping (two harvests per year) with higher water demand became more widespread[14]. However, the impacts of climate change and changes in land management on the changes in crop water consumption in the irrigated areas of Central Asia remain underexplored.

We assess the spatiotemporal dynamics of crop water consumption for every year from 1987 to 2019 across the Amu Darya Basin (535,000 km^2), the main tributary of the Aral Sea. We model ETa of the growing season (April through October) for all irrigated areas and the three dominant cropping practices (dry season cropping, wet season cropping, and double cropping). We use the Landsat-based Operational Simplified Surface Energy Balance model (SSEBop)[15], that has been successfully applied in other arid and semiarid regions for ETa estimates[16–18]. The model is driven

[1]Department of Catchment Hydrology, Helmholtz Centre for Environmental Research-UFZ, Halle (Saale), Germany. [2]Leibniz Institute of Agricultural Development in Transition Economies (IAMO), Halle (Saale), Germany. [3]Geography Department, Humboldt-Universität zu Berlin, Berlin, Germany. [4]Tashkent Institute of Irrigation and Agricultural Mechanization Engineers (TIIAME), National Research University, Tashkent, Uzbekistan. [5]U.S. Geological Survey Earth Resources Observation and Science (EROS) Center, North Central Climate Adaptation Science Center, Fort Collins, CO, USA. [6]Earth and Life Institute, UCLouvain, Louvain-la-Neuve, Belgium. [7]Research Institute of Environment and Nature Conservation Technologies, Tashkent, Uzbekistan. [8]Integrative Research Institute on Transformations of Human-Environment System (IRI THESys), Humboldt-Universität zu Berlin, Berlin, Germany. ✉e-mail: pena.guerrero@ufz.de

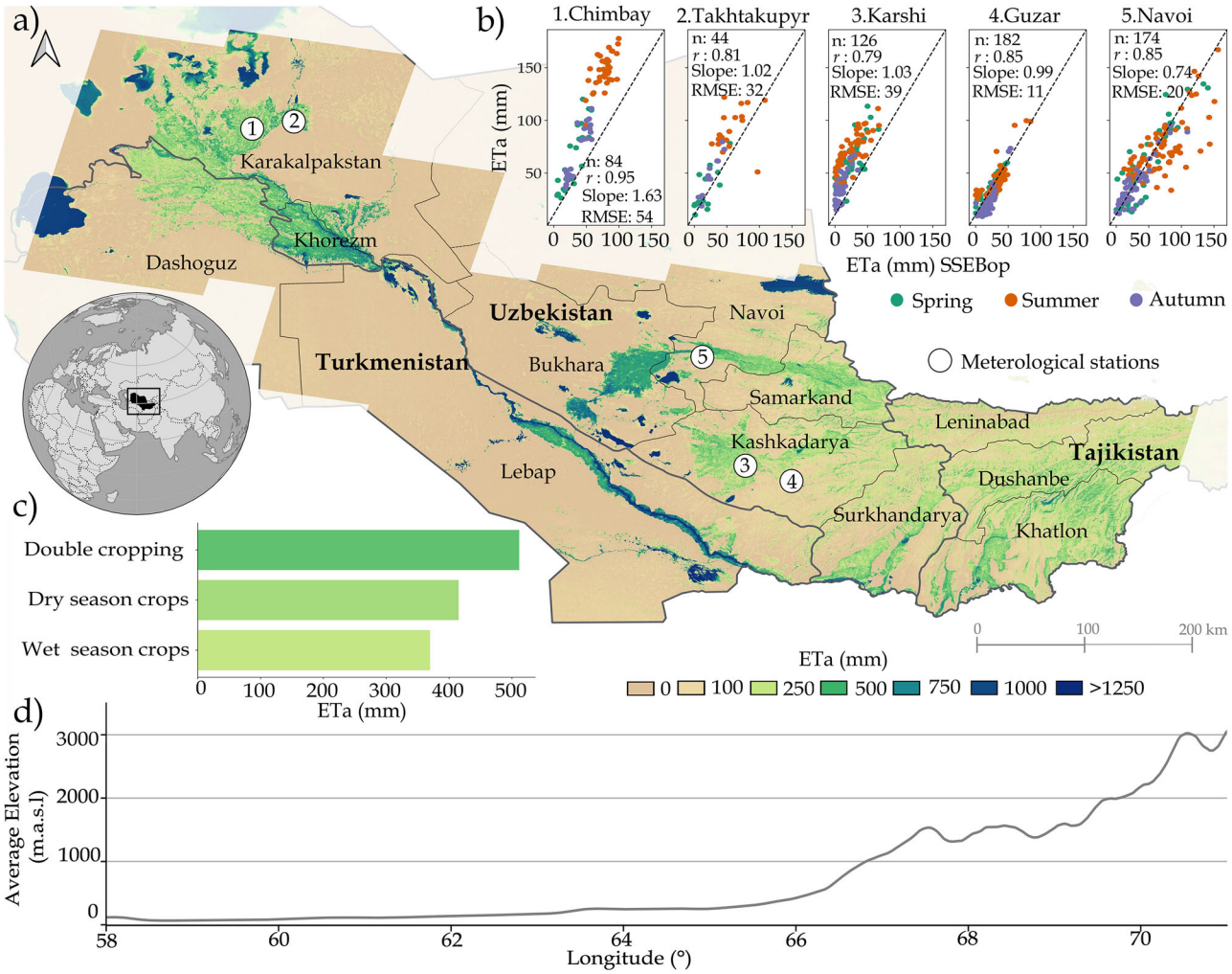

Fig. 1 | Actual evapotranspiration in the Amu Darya Basin. Annual median actual evapotranspiration (ETa) estimates from the SSEBop model during the growing season (April to October) from 1987 to 2019 across all irrigated areas of the Amu Darya Basin. The map has a 30-mspatial resolution (ETa values over 1250 mm/year correspond to open water areas) (**a**). Scatterplots of monthly crop coefficient-based ETa estimates using the Penman-Monteith method based on meteorological data (temperature, wind speed, and relative humidity) and Landsat-derived normalized difference vegetation index (NDVI) from five meteorological stations (Table S3) compared against the SSEBop ETa. The dashed line represents the 1:1 relationship. Root mean square error (RMSE) is expressed in mm/month (**b**). Median annual ETa estimates from SSEBop aggregated by cropping practice (**c**). The topographical profile of the study area is the mean elevation across each degree of longitude at 30-m resolution[22]. The elevation profile was smoothed using a 1000-pixel moving window average across the longitude axis (**d**). The locator map was generated using Cartopy[71] with Natural Earth base layers[72].

by land surface temperature (LST) from Landsat imagery[19] and reference evapotranspiration (PET)[20]. The model is parameterized by the Normalized Difference Vegetation Index (NDVI) from Landsat[19], daily maximum air temperature, net radiation from ERA5-Land, the land component of the fifth generation of the European Centre for Medium-Range Weather Forecasts (ECMWF) atmospheric reanalysis (ERA5)[21], and elevation from the Shuttle Radar Topographic Mission (STRM)[22]. Our annual ETa estimates provide a long-term, high-resolution analysis of crop water consumption in the Amu Darya Basin. These estimates further allow us to disentangle the contribution of land use change and climate change to the changes in crop water consumption.

Results

Actual evapotranspiration in the Amu Darya Basin

We observed the highest crop water consumption in midstream and downstream areas of the Amu Darya Basin where intensive irrigated agriculture dominates (Fig. 1a, d). Stratifying average ETa by cropping practice, we find the highest average crop water consumption for double cropping (511 mm/year), followed by dry season cropping (415 mm/year) and wet season cropping (370 mm/year) (Fig. 1c). Our SSEBop simulations agree with crop coefficient-based ETa estimates from weather stations located in irrigated areas (r ranges from 0.79 to 0.95, RMSE is 11–54 mm/month, with higher differences at lower altitudes and in drier conditions) (Fig. 1b).

Dynamics of crop water consumption

Crop water consumption of wet season cropping exhibited a sharp rise of more than 200% (Fig. 2a) over the study period (calculated as the difference between the average of 1987–1990 and 2016–2019), driven by the expansion of wet season cropping. Still, dry season cropping consumed the most water in terms of volume (7.8 km^3), compared with wet season cropping (3.1 km^3) and double cropping (3.8 km^3) in 2019. The total crop water consumption has risen by 10% over the study period (Fig. 2b). At the 30-meter pixel level (Fig. 2c), average crop water consumption increased for all cropping practices. Dry season crops showed the highest rise in average ETa at 22%, followed by wet season crops at 17% and double cropping at 16% (difference between the average of 1987–1990 and 2016–2019). The basin-wide average ETa increased by 18% (Fig. 2d).

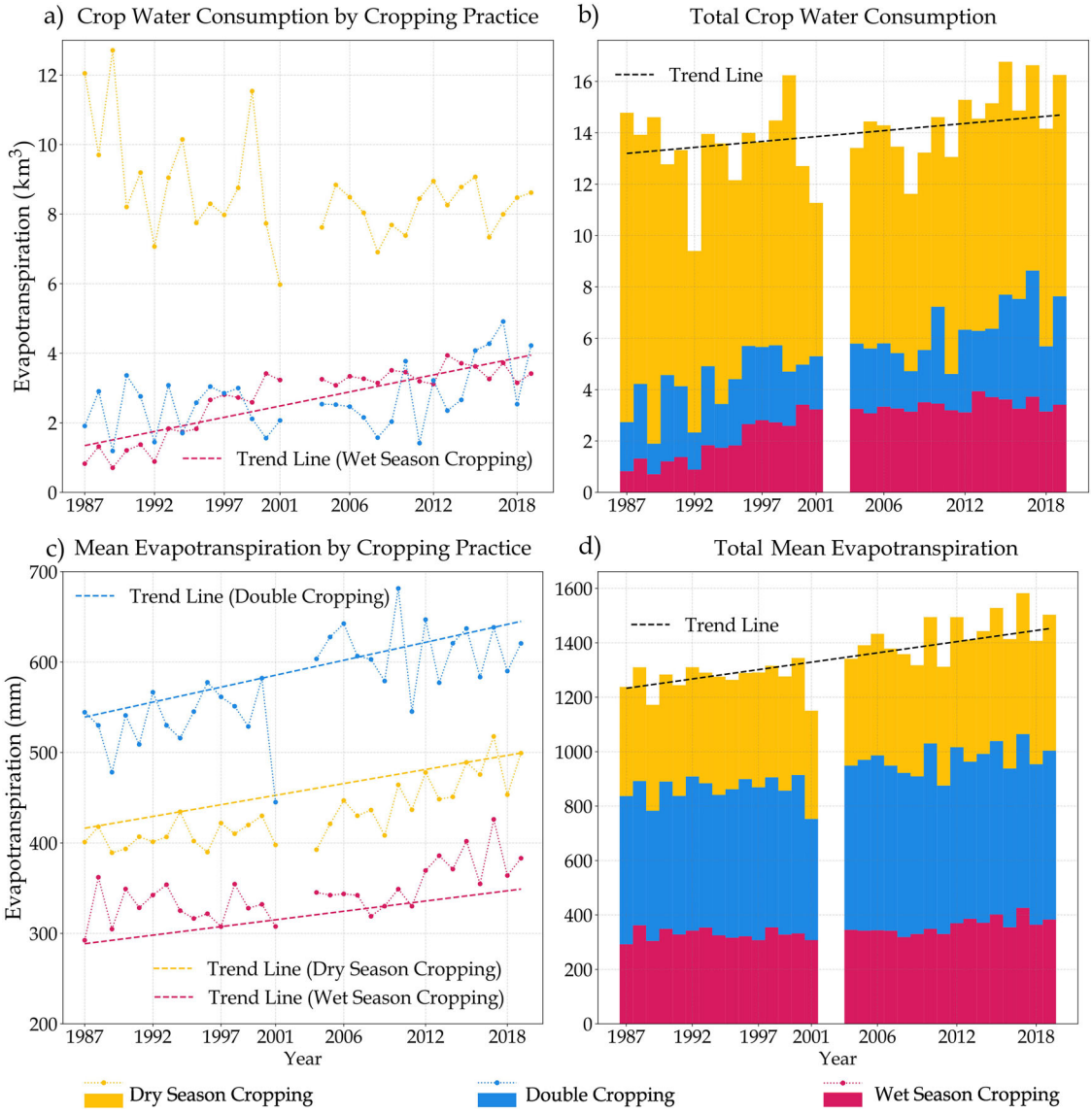

Fig. 2 | Dynamics of crop water consumption in the Amu Darya Basin. Crop water consumption estimated as actual evapotranspiration (ETa) in the Amu Darya Basin for the period 1987-2019. Annual values of crop water consumption for each cropping practice (dry season cropping, double cropping, wet season cropping) are expressed in km^3 (**a**) and stacked to obtain the total volume of the three cropping practices for the entire region, showing an increasing trend (black dashed line, $p = 0.023$) (**b**). Average crop water consumption per pixel for the three main cropping practices, expressed in mm (**c**) and stacked for all cropping practices, shows an increasing trend (black dashed line, $p < 0.001$) (**d**). Dashed lines show significant trends ($p < 0.05$), estimated with the non-parametric Mann–Kendall test and the Theil-Sen estimator, represent the change over time. We excluded the years 2002 and 2003 from the ETa estimates due to insufficient availability of Landsat images, which resulted in high uncertainties of actual evapotranspiration (Supplementary Fig. S1[14]).

Climate drivers and anomalies in crop water consumption

We examined the temporal trends of precipitation, atmospheric water demand (ET reference), and maximum air temperature for downstream, midstream, and upstream regions of the Amu Darya Basin (Figs. 3a, 1–3). ET reference (2.45–4.55 mm/year, $p < 0.001$) and maximum air temperatures (0.04–0.06 °C/year, $p < 0.05$) exhibit a steady increase throughout the study period across all regions. Higher rates of change in maximum temperature and atmospheric water demand occurred in the downstream region compared to the midstream and upstream sections. These changes indicate severe water stress conditions in the downstream areas, particularly during dry years (Fig. 3b).

At the pixel level, downstream regions experienced greater annual ETa anomalies. Values can drop 50% below the median, especially during extremely dry years, such as in Karakalpakstan province (e.g., 2001, Fig. 3b). We also observed higher spatial heterogeneity of anomalies in normal and dry years, where neighboring agricultural fields can experience contrasting ETa anomalies that might be related to different water management practices and water availability. The basin-wide and regional ETa (Figs. S2.1–4) exhibited positive anomalies from 2004 onwards, indicating increased crop water consumption.

Disentangling the contribution of climate and land use to changes in crop water consumption

We used a decomposition approach to attribute the contributions of climate and land use changes to the observed changes in crop water consumption, based on area-weighted ETa[23,24]. We compared the average ETa of a baseline period (1987–1990) with that of the recent period (2016–2019). After 2004, climate change increasingly dominated the rising crop water consumption (Fig. S4). Overall, we found that climate change contributed 21% while land use change offset crop water consumption by 3%, resulting in a net increase of 18% (Fig. 4a).

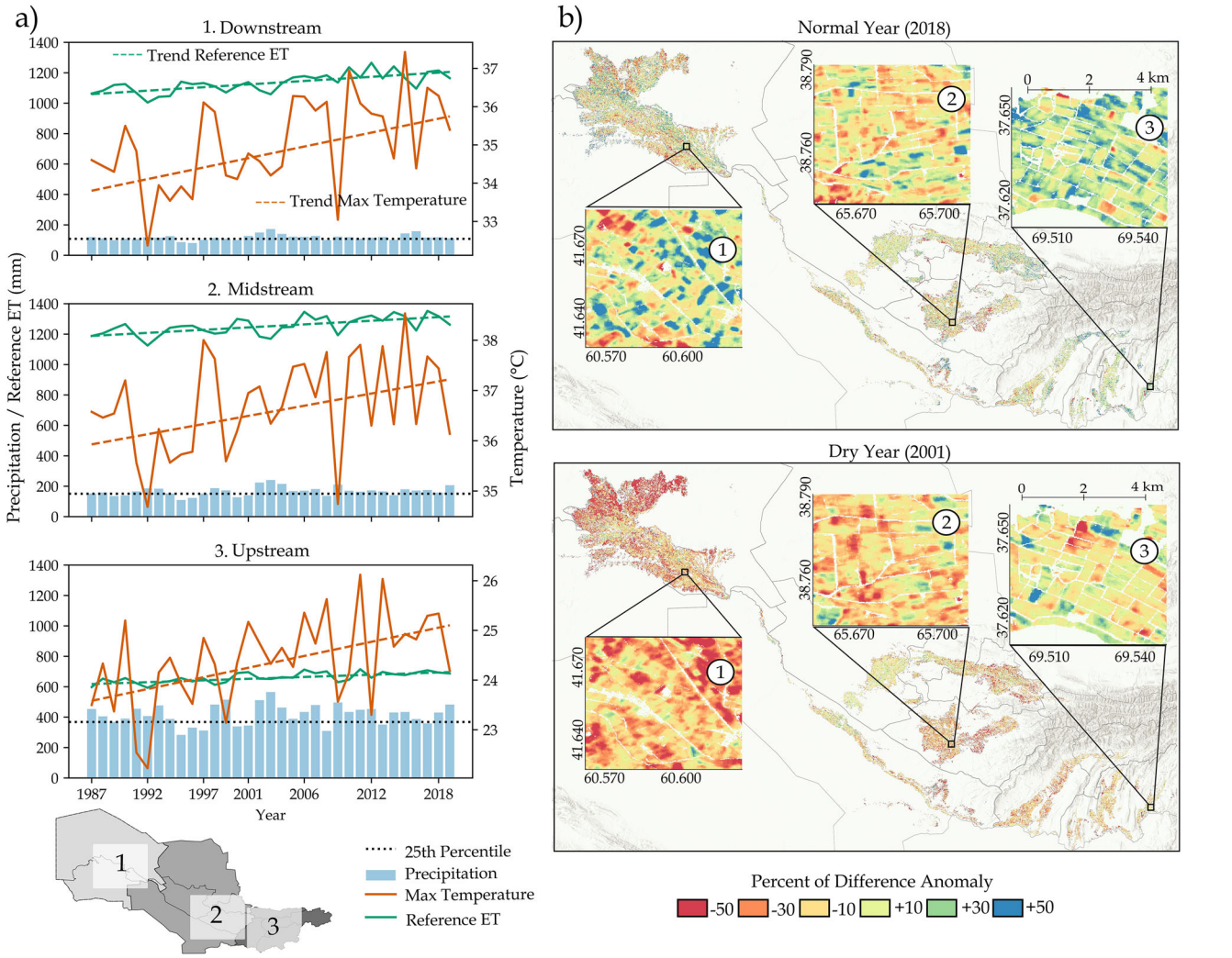

Fig. 3 | Climatic drivers and anomalies of actual evapotranspiration in the Amu Darya Basin. Annual precipitation and maximum air temperature (Max Temperature) and reference evapotranspiration (Reference ET) during the growing season (April to October) for downstream, midstream, and upstream regions (note the different scaling on the y-axis for maximum temperature in the upstream region). The black dashed line represents the 25th percentile of precipitation for each area and is used to classify dry years, defined as those falling below this threshold. Colored dashed lines show significant trends (p <0.05) estimated with the non-parametric Mann–Kendall test and the Theil-Sen estimator to represent their change over time (**a**, 1–3). Anomalies of actual evapotranspiration are expressed as the percent deviation from the median for dry (2001) and normal years (2018) (**b**).

The offset effect varied across the basin (Fig. 4b). The upstream and midstream regions exhibited the most substantial compensatory effects from land use changes. In contrast, land use changes did not compensate for rising water demand downstream, where the increase in ETa was the highest (21%). Although dry season cropping decreased by 25% downstream, it still occupies 60% of the total cropping area, resulting in high water stress conditions amidst accelerating climate change. The 5% offset effect of land use change in the midstream region results from the pronounced changes in the cropping practices away from water-intensive cultivation practices (Fig. S5). Dry season cropping in this region decreased by 40%, while the share of wet season cropping expanded from 13% baseline to 36% in the recent period (2016–2019).

Discussion

Our analysis reveals that, despite the shift toward less water-intensive crops, crop water consumption in the Amu Darya Basin, proxied with ETa, has increased by 10%. Rising atmospheric water demand and increasing temperatures caused the overall and per unit area increase in crop water consumption for all cropping classes. These findings are consistent with global trends of increasing evapotranspiration observed from 1982 to 2010 caused by rising temperatures[25] and higher atmospheric evaporative demand both globally and regionally[26,27]. Similar climate-induced increases in global crop water consumption have been reported for staple crops between 1981 and 2013, with wheat-growing areas experiencing the largest increase[28].

Our decomposition analysis revealed that land use changes mitigated 3% of the potential 21% increase in crop water consumption due to climate change, resulting in a net observed increase of 18%. Dry season crops remain the highest water consumers by total volume, but their overall water consumption has remained constant over the last 20 years. Yet, the increasing crop water consumption due to the expansion of wet season crops and double cropping, and the higher use per unit area contributed to the overall increase of crop water consumption. Importantly, these changes in crop water consumption occurred without expansion of total cropland area (Fig. S6)[14].

The spatial heterogeneity of the changes in crop water consumption mirrors the pivotal role of environmental conditions, irrigation infrastructure, and water governance in shaping regional patterns of crop water use. The midstream region exhibited the highest reduction of water use due to land use change, thanks to the largest shift from dry season (mainly

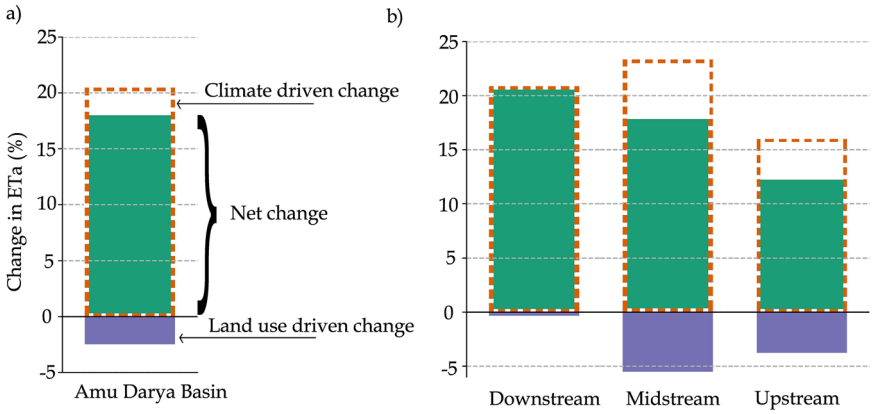

Fig. 4 | Climate and land use contributions to changes in crop water consumption. Net change (green) in actual evapotranspiration (ETa) (comparing the mean of 1987–1990 and 2016–2019) for the Amu Darya Basin expressed in percentage (%), the contribution of land use change (purple), and the potential contribution of climate change (dashed orange) (**a**). Net change for downstream, midstream, and upstream regions (**b**). Stream locations are shown in Fig. 3, and sensitivity analysis using different start and end dates is provided in Fig. S3.

cotton) to wet season (mainly winter wheat) cropping. Besides, midstream areas benefit from more reliable water availability and better soil quality, allowing for greater agricultural diversification[29]. Conversely, downstream areas where water-intensive dry season crops continue to dominate witnessed the highest increase in ETa. These areas, which include intensively irrigated regions, such as Khorezm, Karakalpakstan, and Dashoguz (Fig. 1), face higher salinity, shallow groundwater levels, and less favorable irrigation infrastructure, limiting their capacity for transitioning to less water-intensive crops[30–32].

Governments in Uzbekistan and Turkmenistan retained aspects of the central planning system from the Soviet period, such as controlling crop choices and cultivated area, and imposing cotton production quotas because cotton remained a vital component of their economies[33]. The centralization disproportionately affected downstream regions, which continued to be burdened with cotton production quotas despite escalating land degradation, rising temperatures along with more frequent heat extremes, and growing water scarcity[34,35]. However, successful transitions in regions like Australia demonstrate that, even under challenging conditions, targeted land use changes can help mitigate climate impacts[36]. While our findings underscore that climate change is the dominant driver of increasing ETa, additional factors, such as an increase in applied irrigation water, may also contribute to observed trends in crop water consumption. This study provides a robust framework for quantifying climate-driven changes; future research could advance this understanding by incorporating water balance assessments alongside remote sensing and in-situ observations to disentangle the relative influence of additional water inputs on ETa trajectories.

Key strategies recognized by Central Asian governments focus on increasing crop diversification by introducing alternative crops in planned rotations, alongside adopting conservation agriculture, to mitigate environmental degradation and sustain production[37]. Balanced approaches are needed that integrate efficient irrigation schemes, cropping schedules adapted to water availability, and crops with higher crop water productivity. More efficient irrigation management is essential to support these practices, yet challenges such as aging infrastructure and low water productivity hinder more sustainable crop production[37]. Precision agriculture, deficit irrigation, and drought-tolerant crops offer solutions[38,39], but their success depends on resilient institutions and effective coordination to ensure sustainable water allocation and policy implementation. The collapse of Soviet-era irrigation systems has fueled conflicts over transboundary water resources, exacerbating salinization and desertification while limiting land rehabilitation efforts[40,41]. Recent governance reforms in Central Asia have sought to improve institutional capacity and irrigation efficiency; however, ongoing political tensions, infrastructure deficiencies, and limited integration of scientific research into policy decisions continue to hinder progress toward sustainable water management[42].

Remote sensing has become a valuable tool for water management and agricultural decision-making. By providing spatially detailed and temporally consistent data on ETa, models like the SSEBop reveal water consumption, water use efficiency, and irrigation performance. These insights can inform strategic planning and monitoring in water-stressed areas, such as the Aral Sea Basin[43]. However, challenges remain in estimating irrigation losses and integrating remote sensing data with in-situ observations to better comprehend changes in water availability trends[41,44]. In Central Asia, aging irrigation systems cause significant water conveyance losses, which are rarely integrated into long-term water availability studies[37]. Moreover, the reliance of the region on glacial and snowmelt runoff, which is increasingly affected by climate change, underscores the urgency of improving water management strategies[13,45]. Combining the technological advances of remote sensing applications with robust governance frameworks and transboundary cooperation is essential for sustainable water use[40].

Improved cropping practices, more efficient irrigation systems, better monitoring, and governance reforms are critical for achieving more sustainable water and food systems in Central Asia. However, these efforts alone will not be sufficient without a global commitment to reducing emissions. In 2024, the average global temperature surpassed 1.5 °C above pre-industrial levels, with each of the past 10 years (2015–2024) ranking among the warmest on record[46]. Despite the Paris Agreement signed by 200 countries to limit global warming to 1.5 °C, carbon emissions from fossil fuels and other sources have continued to rise[47]. This highlights the urgency of preparing for critical warming thresholds and higher evapotranspiration rates, requiring stronger mitigation and adaptation strategies[48].

Conclusions

Our study highlights the importance of integrated strategies to ensure the long-term sustainability of agriculture and water management in Central Asia. Despite shifts toward less water-intensive crops, the rising atmospheric water demand, increasing temperatures, and cropping intensification continue to drive higher water consumption. Downstream regions are particularly affected by environmental constraints and aging irrigation infrastructure, which exacerbate the challenges posed by climate change. Land use changes can only provide modest mitigation of water scarcity, amidst accelerating climate change and persistent inefficiencies in irrigation systems.

To achieve sustainable water and food systems, it is imperative to address critical research gaps, including assessing the relative influence of additional water inputs on ETa trends, quantifying irrigation losses, and integrating water availability trends across time and space. Enhancing governance frameworks, fostering transboundary cooperation, and modernizing irrigation infrastructure will be essential to balance agricultural productivity with resource conservation. However, local measures alone cannot fully counter the intensifying impacts of a warming climate. Without a meaningful reduction in global emissions, even well-designed regional interventions risk being overshadowed by broader global climatic shifts. For Central Asia, ambitious global action is essential for building resilience in water and agricultural systems.

Methods

Data and methods

Study area. The present study was conducted in the Amu Darya Basin, covering 535,000 km^2 from the Tien Shan and Pamir Mountains to the downstream drylands of Tajikistan, Turkmenistan, and Uzbekistan (Fig. 1a). The Amu Darya is the largest river in Central Asia and the primary source of freshwater. The river depends on the water storage in snow and ice from the headwater catchments of the mountains[49–51]. The basin has a highly continental climate with hot, dry summers and cold, wet winters. Average precipitation in the region ranges from 50 mm/year in the desert regions to 1000 mm/year in the mountains. Temperature has a strong diurnal and intra-annual variation from −40 °C (minimum air temperature in winter) to above 40 °C (maximum air temperature in summer). Over 90% of the water withdrawals in the region are used for irrigation[52,53]. Irrigated crop production focuses on cereals (mainly wheat) cultivated during the wet season (winter) and cotton with a growing period during the hot and dry summer season. The share of fodder and permanent crop cultivation tends to increase with elevation[54,55].

Data. For every year of our study period, we isolated the agricultural lands of the Amu Darya using the Landsat-based cropland maps at 30-m spatial resolution of the Amu Darya Basin[14]. These maps were used to extract the spatial extent and the actual evapotranspiration of the three cropping practices (Wet season cropping, dry season cropping, and double cropping) (Supplementary Table S1). To analyze the temporal trends of the climate drivers, we used daily precipitation from the Climate Hazard Group InfraRed Precipitation with Station Data (CHIRPS version 2) with a spatial resolution of 0.05° (about 5 km at the equator)[56], which was considered most accurate for the region[57]. We also obtained daily maximum air temperature from the global reanalysis ERA5-Land with 0.1° (about 9 km at the equator) of spatial resolution[21], and for reference evapotranspiration we used the Potential Evapotranspiration (PET) dataset at a daily scale with 0.1° of spatial resolution[20]. For trend detection, we employed the non-parametric Mann–Kendall test and the Theil–Sen estimator, both implemented in the pyMannKendall Python package[58].

Modeling of actual evapotranspiration. We used the Operational Simplified Surface Energy Balance (SSEBop) model in the Google Earth Engine (GEE)[59] cloud computing platform[43], along with Python and Quantum GIS (QGIS). SSEBop computes daily total actual evapotranspiration (ETa) using a combination of LST from Landsat and reference ET. We used Landsat collection 2 Tier 1 surface reflectance products[19] covering the irrigated agriculture of the Amu Darya Basin during the growing season (April to October) between 1987 and 2019. We only used images with less than 60% cloud cover. In total, 9511 Landsat images were collected, with 42% of the images coming from Landsat 7 (3961), 39% from Landsat 5 (3779), 18% from Landsat 8 (1695), and 1% from Landsat 4 (76). The median number of clear-day images per year was 12 (see Fig. S7). For grass reference evapotranspiration (ET_o), we used PET, which was calculated via the FAO's Penman-Monteith method[60]. The model also uses as ancillary datasets daily maximum temperature from ERA5-Land and digital elevation model (DEM, 30-m) from the Shuttle Radar Topography Mission (SRTM)[22] (See Supplementary Table S2).

SSEBop is a parametric energy balance model that solves the latent heat flux at a daily time scale using a satellite psychrometric approach[61]. Daily ETa is calculated as the product of ET fraction (ETf) and reference ET[15]. The difference between the dry-bulb (observed LST) and wet-bulb reference LST determines the ETf in combination with a surface psychrometric constant. The SSEBop model integrates input datasets at their native resolution, with the spatial resolution of the final ETa output determined by the thermal input (LST). Coarser-resolution inputs such as reference ET and air temperature are treated as regional variables, which vary slowly in space and are suitable for integration without resampling, following common practice in thermal-based ET modeling. We used the open-access SSEBop FANO (v.0.2.8) Python implementation[62]. The model implementation includes an improved parameterization using the Forcing and Normalizing Operation (FANO) algorithm[44]. This algorithm increases the spatiotemporal coverage of ETa estimations in all landscapes and seasons, regardless of vegetation cover density in comparison with previous versions. ET fractions (ETf) from satellite overpass dates are linearly interpolated to create daily ETf that are multiplied with the corresponding ETo to create daily total ETa which in turn are aggregated to monthly and summed for our period of interest: 1 April to 31 October for all years from 1987 to 2019. All resulting maps are openly available for further use at https://doi.org/10.5281/zenodo.17720311.

Performance evaluation. We evaluated the SSEBop model by comparing its monthly estimates with the commonly used crop coefficient-based (Kc) ET approach[63], which combines NDVI and reference evapotranspiration derived from meteorological observations (net radiation, temperature, wind speed, pressure, and relative humidity) to estimate crop water use under optimal, well-watered conditions. Kc-based comparison was conducted at five weather stations, located in irrigated areas of Kashkadarya, Navoi, and Karakalpakstan provinces in Uzbekistan (Fig. 1, Supplementary Table S3). The station data were collected from local research and governmental institutions. While the number and spatial distribution of the stations are limited due to data availability in this region, the performance evaluation prioritizes the consistency of ETa estimates across space and time, rather than absolute accuracy. The Kc-based method serve as the upper boundary for crop ET. Thus, SSEBop ETa is expected to be lower (under water stress) than or similar (under optimal conditions) to the Kc-based estimate for each station. We first estimated grass reference evapotranspiration (ETo) using the standardized Penman-Monteith equation (Eq. 1) for each station:

$$ETo = \frac{0.408\left(R_N - G_0\right) + \gamma \frac{900}{T_{a+273}} + u_2(e_s - e_a)}{\Delta + \gamma(1 + 0.34u_2)} \quad (1)$$

where u_2 is wind speed at 2 m height [m s^{-1}], e_s is the saturation vapor pressure (kPa), e_a to the actual vapor pressure (kPa), Δ is the slope of the vapor pressure [kPa °C^{-1}], R_N is the net radiation at the crop surface [MJ m^{-2} day^{-1}], G_0 is the soil heat flux density [MJ m^{-2} day^{-1}], and T_a is the mean daily air temperature at 2 m height (°C). We estimated the Penman-Monteith reference evapotranspiration using the PyET package[64,65]. We then used the Landsat-derived monthly NDVI to estimate the Kc-based ETa (Eq. 2)[63].

$$ETa = 1.25\,NDVI * ETo \quad (2)$$

We evaluated the SSEBop ETa estimates by averaging the values of all pixels within a 100 m radius circular buffer around each station and comparing them with the Kc-based ETa at weather station sites using Pearson correlation, slope, and root mean square error (RMSE) using Scikit-learn[66,67].

To verify that the observed trends were not an artefact of varying data availability, we assessed the relationship between the maximum time gap in clear Landsat observations and the maximum residuals of estimated ETa at the reference sites. This analysis confirmed the absence of any systematic relationship (Fig. S8).

Uncertainty considerations. Remote sensing-based ET estimations have demonstrated good accuracy for water management applications, with a recent evaluation of six OpenET models, including SSEBop, against 139 eddy covariance flux towers in the United States[68]. Growing season ET was estimated with an average percent mean bias error (% MBE), percent root mean square (%RMSE) and $r2$ of −2.1%, 19.8%, and 0.87, respectively, for the Ensemble, with individual models ranging from

0.5 to 7.6 (%MBE), 18.5 to 20.7 (%RMSE), 0.79 to 0.84 ($r2$)[69]. As part of the OpenET Ensemble, the SSEBop model was evaluated with −2.1% (%MBE), 19.8 (%RMSE), and 0.82 ($r2$). Earlier evaluation reported the uncertainties or random errors from input variables and model parameters of the SSEBop led to monthly ET estimates with relative errors less than 20% across multiple flux tower sites distributed across different biomes in the United States[70].

Decomposition analysis. Decomposition analysis (DA) allows us to distinguish the effects of climate and land use changes on crop water consumption. We adapted a methodological approach from previous studies[23,24] and incorporated land use change through an area-weighted ETa method. DA decomposes the change in ETa into two components: climate change and land use effects. To mitigate interannual variability, we compared average ETa over a *baseline period* (1987–1990) with the average ETa during a more *recent period* (2016–2019).

The total change in ETa (ΔETa) is a sum of climate-induced change ($\Delta ETa_{climate}$) and a change induced by land use ($\Delta ETa_{landuse}$):

$$\Delta ET_a = \Delta ETa_{climate} + \Delta ETa_{landuse} \quad (3)$$

The contribution due to climate change is estimated by calculating how much evapotranspiration per pixel has changed for each crop class, weighted by crop class baseline area:

$$\Delta ETa_{climate} = \frac{\sum_i A_{i,baseline}\, x\, (ETa_{i,recent} - ETa_{i,baseline})}{\sum_i A_{i,baseline}}, \text{ where} \quad (4)$$

A_i – is the area under crop class $_i$ so that $i \in$ *{dry season, wet season, double cropping}*,

$ETa_{i,\ baseline}$ – is ETa of crop class $_i$ in the baseline period,

$ETa_{i,\ recent}$ – is ETa of crop class $_i$ in the recent period.

The contribution due to land use change is estimated by comparing the average ETa in the recent period to what it would have been if the crop structure had been maintained as in the baseline period:

$$\Delta ETa_{landuse} = \frac{\sum_i A_{i,recent} * ETa_{i,recent}}{\sum_i A_{i,recent}} - \frac{\sum_i A_{i,baseline} * ETa_{i,recent}}{\sum_i A_{i,baseline}} \quad (5)$$

The additive framework of this decomposition method assumes linearity and does not capture potential interaction between drivers. While climate change may influence land use decisions in other regions, such interactions are considered negligible in the Amu Darya Basin, where irrigation is the primary determinant of agricultural land use.

We conducted a sensitivity analysis (Fig. S3) to confirm that the results remain consistent regardless of how the baseline and recent periods are defined in terms of the number of years.

Data availability

The annual ETa dataset generated in this study is publicly available on Zenodo at: https://doi.org/10.5281/zenodo.17720311. All input datasets used for modeling ETa are publicly available, including Landsat Collection 2 surface reflectance products (https://www.usgs.gov/landsat-missions/landsat-collection-2-surface-reflectance), the SRTM digital elevation model (https://doi.org/10.1029/2005rg000183), ERA5-Land climate reanalysis data (https://doi.org/10.1002/qj.3803), and the PET reference evapotranspiration dataset (https://doi.org/10.1038/s41597-021-01003-9). The meteorological station data used for the validation analysis were obtained from regional research and governmental institutions in Uzbekistan. These datasets cannot be redistributed publicly, but they may be available from the authors upon reasonable request.

Code availability

The ETa estimates were generated using the open-source SSEBop FANO (v0.2.8) implementation provided by the OpenET project (https://github.com/Open-ET/openet-ssebop).

Received: 15 April 2025; Accepted: 16 December 2025;
Published online: 08 January 2026

References

1. Food and Agriculture Organization (FAO)s. AQUASTAT Database https://data.apps.fao.org/aquastat/?lang=en, (2021).
2. Mehta, P. et al. Half of twenty-first century global irrigation expansion has been in water-stressed regions. *Nat. Water* **2**, 254–261 (2024).
3. Intergovernmental Panel on Climate Change (IPCC). Climate Change 2022 – Impacts, Adaptation and Vulnerability. (eds Pörtner, H.-O. et al.). Working Group II Contribution to the Sixth Assessment Report of the Intergovernmental Panel on Climate Change. (Cambridge University Press, 2022). https://doi.org/10.1017/9781009325844.
4. Wang-Erlandsson, L. et al. A planetary boundary for green water. *Nat. Rev. Earth Environ.* https://doi.org/10.1038/s43017-022-00287-8 (2022).
5. Qin, Y. et al. Flexibility and intensity of global water use. *Nat. Sustain.* **2**, 515–523 (2019).
6. Jasechko, S. et al. Terrestrial water fluxes dominated by transpiration. *Nature* **496**, 347–350 (2013).
7. Bawa, A., Senay, G. B. & Kumar, S. Regional crop water use assessment using Landsat-derived evapotranspiration. *Hydrol. Process.* **35**, https://doi.org/10.1002/hyp.14015 (2020).
8. Dembélé, M. et al. Potential of satellite and reanalysis evaporation datasets for hydrological modelling under various model calibration strategies. *Adv. Water Resour.* **143**, https://doi.org/10.1016/j.advwatres.2020.103667 (2020).
9. Senay, G. B. et al. Long-Term (1986–2015) crop water use characterization over the Upper Rio Grande Basin of United States and Mexico Using Landsat-Based Evapotranspiration. *Remote Sens.* **11**, https://doi.org/10.3390/rs11131587 (2019).
10. Mannig, B. et al. Dynamical downscaling of climate change in Central Asia. *Global Planet Change* **110**, 26–39 (2013).
11. Yapiyev, V., Sagintayev, Z., Inglezakis, V., Samarkhanov, K. & Verhoef, A. Essentials of Endorheic basins and lakes: a review in the context of current and future water resource management and mitigation activities in Central Asia. *Water* **9**, https://doi.org/10.3390/w9100798 (2017).
12. White, K. D. A geographical perspective on the Aral Sea crisis: three interpretations of an image. *Bull. Geogr. Socio-econ. Ser.* **21**, 125–132 (2013).
13. Micklin, P. et al. "The Aral Sea: A Story of Devastation and Partial Recovery of a Large Lake." In Large Asian Lakes in a Changing World, edited by S. Mischke. Cham: Springer. https://doi.org/10.1007/978-3-030-42254-7_4, 2020.
14. Rufin, P., Peña-Guerrero, M. D., Umirbekov, A., Wei, Y. & Müller, D. Post-Soviet changes in cropping practices in the irrigated drylands of the Aral Sea basin. *Environ. Res. Lett.* **17**, 095013 (2022).
15. Senay, G. B. et al. Operational evapotranspiration mapping using remote sensing and weather datasets: a new parameterization for the SSEB approach. *JAWRA J. Am. Water Resour. Assoc.* **49**, 577–591 (2013).
16. Jin, X., Zhu, X. & Xue, Y. Satellite-based analysis of regional evapotranspiration trends in a semi-arid area. *Int. J. Remote Sens.* **40**, 3267–3288 (2019).
17. Olivera-Guerra, L. et al. An operational method for the disaggregation of land surface temperature to estimate actual evapotranspiration in the arid region of Chile. *ISPRS J. Photogrammetry Remote Sens.* **128**, 170–181 (2017).
18. Filippelli, S. K. et al. Remote sensing of field-scale irrigation withdrawals in the central Ogallala aquifer region. *Agric. Water Manag.* **271**, https://doi.org/10.1016/j.agwat.2022.107764 (2022).

19. U.S. Geological Surveys. Landsat Collection 2 Level-2 Science Products (https://www.usgs.gov/landsat-missions/landsat-collection-2-surface-reflectance, 2020).
20. Singer, M. B. et al. Hourly potential evapotranspiration at 0.1 degrees resolution for the global land surface from 1981-present. *Sci Data* **8**, 224 (2021).
21. Hersbach, H. et al. The ERA5 global reanalysis. *Quart. J. R. Meteorol. Soc.* **146**, 1999–2049 (2020).
22. Farr, T. G. et al. The shuttle radar topography mission. *Rev. Geophys.* **45**, https://doi.org/10.1029/2005rg000183 (2007).
23. Wang, D. & Hejazi, M. Quantifying the relative contribution of the climate and direct human impacts on mean annual streamflow in the contiguous United States. *Water Resour. Res.* **47**, https://doi.org/10.1029/2010wr010283 (2011).
24. Renner, M. & Hauffe, C. Impacts of climate and land surface change on catchment evapotranspiration and runoff from 1951 to 2020 in Saxony, Germany. *Hydrol. Earth Syst. Sci.* **28**, 2849–2869 (2024).
25. Mao, J. et al. Disentangling climatic and anthropogenic controls on global terrestrial evapotranspiration trends. *Environ. Res. Lett.* **10**, https://doi.org/10.1088/1748-9326/10/9/094008 (2015).
26. Vicente-Serrano, S. M. et al. Global drought trends and future projections. *Philos. Trans. A Math Phys. Eng Sci.* **380**, 20210285 (2022).
27. Xu, H. -j, Wang, X. -p & Zhang, X. -x Decreased vegetation growth in response to summer drought in Central Asia from 2000 to 2012. *Int. J. Appl. Earth Observ. Geoinform.* **52**, 390–402 (2016).
28. Urban, D. W., Sheffield, J. & Lobell, D. B. Historical effects of CO2 and climate trends on global crop water demand. *Nat. Clim. Change* **7**, 901–905 (2017).
29. FAO. AQUASTAT Country Profile – Uzbekistan. (Food and Agriculture Organization of the United Nations (FAO), Rome, Italy, 2012). https://www.fao.org/aquastat/en/countries-and-basins/country-profiles/country/UZB.
30. Ibrakhimov, M., Martius, C., Lamers, J. P. A. & Tischbein, B. The dynamics of groundwater table and salinity over 17 years in Khorezm. *Agric. Water Manag.* **101**, 52–61 (2011).
31. Dubovyk, O. *Multi-scale targeting of land degradation in northern Uzbekistan using satellite remote sensing*, Rheinischen Friedrich-Wilhelms-Universität Bonn, https://doi.org/10.13140/RG.2.1.1826.3205, (2013).
32. Abdullaev, I. & Rakhmatullaev, S. Central Asian irrigation sector in a climate change context: some reflections. *J. Water Clim. Change* **5**, 341–356 (2014).
33. Pomfret, R. Distortions To Agricultural Incentives in Tajikistan, Turkmenistan and Uzbekistan. in *Distortions to Agricultural Incentives in Eastern Europe and Central Asia*, (eds Anderson, K. & Swinnen, J) (World Bank, 2009).
34. Spoor, M. The Aral sea basin crisis: transition and environment in former Soviet Central Asia. *Dev. Change* **29**, 409–435 (1998).
35. O'hara, S. L. Lessons from the past: water management in Central Asia. *Water Policy* **2**, 365–384 (2000).
36. Kirby, M., Bark, R., Connor, J., Qureshi, M. E. & Keyworth, S. Sustainable irrigation: how did irrigated agriculture in Australia's Murray–Darling Basin adapt in the Millennium Drought?. *Agric. Water Manag.* **145**, 154–162 (2014).
37. Conrad, C., Usman, M., Morper-Busch, L. & Schönbrodt-Stitt, S. Remote sensing-based assessments of land use, soil and vegetation status, crop production and water use in irrigation systems of the Aral Sea Basin. A review. *Water Security* **11**, 100078 (2020).
38. Geerts, S. & Raes, D. Deficit irrigation as an on-farm strategy to maximize crop water productivity in dry areas. *Agric. Water Manag.* **96**, 1275–1284 (2009).
39. Ahmed, M. et al. Impact of climate change on dryland agricultural systems: a review of current status, potentials, and further work need. *Int. J. Plant Prod.* **16**, 341–363 (2022).
40. Djanibekov, N., Van Assche, K. & Valentinov, V. Water Governance in Central Asia: A Luhmannian Perspective. *Soc. Nat. Resour.* **29**, 822–835 (2015).
41. Hamidov, A., Helming, K. & Balla, D. Impact of agricultural land use in Central Asia: a review. *Agron. Sustain. Dev.* **36**, 6 (2016).
42. Abdullaev, I. et al. Current challenges in Central Asian water governance and their implications for research, higher education, and science-policy interaction *Central*. *Asian J. Water Res.* **11**, 47–58 (2025).
43. Senay, G. B. et al. Mapping actual evapotranspiration using Landsat for the conterminous United States: Google Earth Engine implementation and assessment of the SSEBop model. *Remote Sens. Environ.* **275**, https://doi.org/10.1016/j.rse.2022.113011 (2022).
44. Senay, G. B. et al. Improving the Operational Simplified Surface Energy Balance Evapotranspiration Model Using the Forcing and Normalizing Operation. *Remote Sens.* **15**, https://doi.org/10.3390/rs15010260 (2023).
45. Kraaijenbrink, P. D. A., Stigter, E. E., Yao, T. & Immerzeel, W. W. Climate change decisive for Asia's snow meltwater supply. *Nat. Clim. Change* **11**, 591–597 (2021).
46. Copernicus Climate Change Services. Copernicus: 2024 is the first year to exceed 1.5 °C above pre-industrial level https://climate.copernicus.eu/copernicus-2024-first-year-exceed-15degc-above-pre-industrial-level, (2025).
47. Tollefson, J. Earth breaches 1.5 °C climate limit for the first time: what does it mean?. *Nature* **637**, 769–770 (2025).
48. Bevacqua, E., Schleussner, C.-F. & Zscheischler, J. A year above 1.5 °C signals that Earth is most probably within the 20-year period that will reach the Paris Agreement limit. *Nat. Clim. Change* **15**, 262–265 (2025).
49. Aus der Beek, T., Voß, F. & Flörke, M. Modelling the impact of Global Change on the hydrological system of the Aral Sea basin. *Phys. Chem. Earth, Parts A/B/C* **36**, 684–695 (2011).
50. Krysanova, V. et al. Cross-comparison of climate change adaptation strategies across large river basins in Europe, Africa and Asia. *Water Resour.Manag.* **24**, 4121–4160 (2010).
51. Reyer, C. P. O. et al. Climate change impacts in Central Asia and their implications for development. *Region. Environ. Change* **17**, 1639–1650 (2017).
52. White, C. J., Tanton, T. W. & Rycroft, D. W. The impact of climate change on the water resources of the Amu Darya Basin in Central Asia. *Water Resources Management* **28**, 5267–5281 (2014).
53. AQUASTAT, F.s. AQUASTAT - Global information system on water resources and agricultural water management https://www.fao.org/aquastat/en/, (2023).
54. Food and Agriculture Organization (FAO). Irrigation in Central Asia in Figures – AQUASTAT Survey FAO Water Reports 39. Rome: Food and Agriculture Organization of the United Nations. https://www.fao.org/3/i3289e/i3289e.pdf. (2012).
55. Conrad, C., Schönbrodt-Stitt, S., Löw, F., Sorokin, D. & Paeth, H. Cropping Intensity in the Aral Sea Basin and Its Dependency from the Runoff Formation 2000–2012. *Remote Sensing* **8**, 630 (2016).
56. Funk, C. et al. The climate hazards infrared precipitation with stations-a new environmental record for monitoring extremes. *Sci. Data* **2**, 150066 (2015).
57. Peña-Guerrero, M. D., Umirbekov, A., Tarasova, L. & Müller, D. Comparing the performance of high-resolution global precipitation products across topographic and climatic gradients of Central Asia. *Int. J. Climatol.* **42**, 5554–5569 (2022).
58. Hussain, M. & Mahmud, I. pyMannKendall: a python package for non parametric Mann Kendall family of trend tests. Available from: https://github.com/mmhs013/pyMannKendall, (2019).
59. Gorelick, N. et al. Google Earth Engine: Planetary-scale geospatial analysis for everyone. *Remote Sens. Environ.* **202**, 18–27 (2017).
60. Allen, R. G., Pereira, L. S., Raes, D. & Smith, M. Crop evapotranspiration-Guidelines for computing crop water

requirements-FAO Irrigation and drainage paper 56. (Food and Agriculture Organization of the United Nations, Rome,1998). https://www.fao.org/4/x0490e/x0490e00.htm.
61. Senay, G. B. Satellite Psychrometric Formulation of the Operational Simplified Surface Energy Balance (SSEBop) Model for Quantifying and Mapping Evapotranspiration. *Appl. Eng. Agric.* **34**, 555–566 (2018).
62. OpenET. SSEBop FANO (v0.2.8). 0.2.8. GitHub; Available from: https://github.com/Open-ET/openet-ssebop, (2024).
63. Allen, R. G., Pereira, L. S., Howell, T. A. & Jensen, M. E. Evapotranspiration information reporting: I. Factors governing measurement accuracy. *Agric. Water Manag.* **98**, 899–920 (2011).
64. Vremec, M. & Collenteur, R. PyEt-open source Python package for calculating reference and potential evaporation. 1.2.2. Zenodo; Available from: https://github.com/pyet-org/pyet/tree/v1.4.0, (2024).
65. Vremec, M., Collenteur, R. A. & Birk, S. PyEt v1.3.1: a Python package for the estimation of potential evapotranspiration. *Geosci. Model Dev.* **17**, 7083–7103 (2024).
66. Pedregosa, F. et al. Scikit-learn: Machine Learning in Python. *J. Mach. Learn. Research* **12**, 2825–2830 (2011).
67. scikit-learn developers. scikit-learn: Machine Learning in Python. 1.0.2. Available from: https://scikit-learn.org, (2024).
68. Melton, F. S. et al. OpenET: filling a critical data gap in water management for the Western United States. *J. Am. Water Resour. Assoc.* **58**, 971–994 (2021).
69. Volk, J. M. et al. Assessing the accuracy of OpenET satellite-based evapotranspiration data to support water resource and land management applications. *Nat. Water* **2**, 193–205 (2024).
70. Chen, M., Senay, G. B., Singh, R. K. & Verdin, J. P. Uncertainty analysis of the Operational Simplified Surface Energy Balance (SSEBop) model at multiple flux tower sites. *J. Hydrol.* **536**, 384–399 (2016).
71. Met Office. Cartopy: A cartographic Python package. 0.18.0. Met Office; Available from: https://cartopy.readthedocs.io, 2010-2023.
72. Natural Earth. Free vector and raster map data. Available from: https://www.naturalearthdata.com, (2024).

Acknowledgements

This research was supported by the Volkswagen Foundation through the Sustainable Agricultural Development in Central Asia (SUSADICA) project (Grant No. 96264). We thank Dr. Zafar Gafurov for his support in obtaining meteorological station data. We are also grateful to the two anonymous reviewers for their constructive feedback. Any use of trade, firm, or product names is solely for descriptive purposes and does not imply endorsement by the U.S. Government.

Author contributions

M.D.P.-G. designed the study, developed the evapotranspiration processing workflow, performed the analyses, interpreted the results, and led the writing of the manuscript. G.B.S. advised on the SSEBop methodology, contributed to the interpretation of evapotranspiration modeling results, and revised the manuscript. A.U. contributed regional expertise, supported the study design and interpretation, contributed to the conceptual and methodological development of the study, and revised the manuscript. L.T. contributed to conceptual and methodological development, supported the interpretation of results, and revised the manuscript. P.R. provided the irrigated cropland maps, contributed to the conceptual and methodological development of the study, supported the interpretation of results, and revised the manuscript. B.P. contributed regional expertise, facilitated access to validation data, and revised the manuscript. D.M. supervised the research, contributed to study design and interpretation, and reviewed and edited the manuscript.

Funding

Open Access funding enabled and organized by Projekt DEAL.

Competing interests

The authors declare no competing interests.

Additional information

Supplementary information The online version contains supplementary material available at https://doi.org/10.1038/s43247-025-03142-y.

Correspondence and requests for materials should be addressed to Mayra Daniela Peña-Guerrero.

Peer review information *Communications Earth and Environment* thanks the anonymous reviewers for their contribution to the peer review of this work. Primary Handling Editors: Wenfeng Liu, Aliénor Lavergne, and Mengjie Wang. [A peer review file is available.]